

---

# The Coherent Addition of Gratings for Pulse Compression in High-Energy Laser Systems

## Introduction

Short-pulse, high-energy, and high-irradiance laser systems provide many new opportunities for studies in light–matter interaction and inertial confinement fusion, including x-ray radiography and fast ignition. Research in high-intensity, high-energy backlighting for high-energy-density physics experiments under ignition conditions and integrated fast-ignition experiments with cryogenic targets depend on the development of short-pulse, high-irradiance lasers.<sup>1</sup> High-power, solid-state lasers, using the chirped-pulse-amplification (CPA) scheme, incorporate pulse compressors containing holographic gratings.<sup>2</sup> The most-promising grating technology is a holographically formed grating combined with a multilayer dielectric (MLD) coating to form a highly efficient grating used in reflection.<sup>3–5</sup> The four primary grating requirements, namely high diffraction efficiency, high wavefront quality, large aperture, and high damage threshold, make it a highly constrained optical system. The aperture size and damage threshold of reflection gratings determine the short-pulse energy capability of petawatt laser systems. The critical compressor component is the last grating, which experiences the shortest pulse and therefore the highest power. The highest reported damage threshold for commercially available MLD gratings is  $0.6 \text{ J/cm}^2$  at 275-fs pulse width.<sup>6</sup> Assuming a square root of time scaling, these gratings would have a damage threshold of  $\sim 1.2 \text{ J/cm}^2$  for a 1-ps pulse width. For a grating with 1740 l/mm and a Littrow angle of  $66.5^\circ$  for  $\lambda = 1054 \text{ nm}$ , this surface fluence corresponds to a beam fluence, measured in a plane normal to beam propagation, of approximately  $3 \text{ J/cm}^2$ . These gratings are currently available in approximately 50-cm lengths. Assuming a 1.8 safety factor for diffraction modulation, the above provides an energy of less than 1 kJ. Gratings with larger apertures can further extend the short-pulse energy capability of petawatt laser systems; however, since the difficult fabrication process for MLD reflection gratings may limit the ultimate size of an individual grating to less than 1 m, alternative approaches are critical to scaling toward multiple-kilojoule, short-pulse laser systems.

## Concept Description

The coherent summation of multiple gratings to form a larger grating provides an alternative to meter-sized MLD gratings. We refer to this alternative as grating tiling. A tiled-grating compressor (TGC) is capable of handling greater laser energy than a grating-aperture–limited compressor. For each of the gratings within the compressor,  $N \times M$  sub-aperture gratings can be mounted adjacently to form a larger tiled grating.<sup>7</sup> When properly aligned, they will act as a monolithic optical element. For example, Fig. 96.1 shows a four-grating compressor with each tiled grating containing three sub-aperture gratings. The configuration is being considered for the OMEGA EP laser system. In general, the aperture, and therefore the energy, of a TGC is increased by a factor of  $N \times M$  over that of grating-aperture–limited compressors. Similar to the scheme deployed by the astronomy community to construct very large telescopes<sup>8</sup> using an array of mirrors, large gratings can be assembled from multiple smaller gratings. Accurate control of the position and orientation of the grooves of each grating presents a significantly greater challenge than that associated with mirror arrays. Despite the perceived difficulty, we have developed a far-field–based approach that makes grating tiling practical.<sup>9,10</sup> As shown in Fig. 96.2, there are five degrees of freedom between each adjacent pair of gratings within a tiled-grating system: tip, tilt, rotation, in-plane shift, and out-of-plane shift. However, only three distinct types of optical path differences exist between closely aligned grating pairs. Relative shifts along the  $x$  and  $z$  axes result in a differential piston phase between the grating pairs. Similarly, relative rotations about the  $x$  and  $z$  axes result in a differential tilt phase between the grating pairs. Relative rotation about the  $y$  axis results in an additional tilt, while the relative shift along the  $y$  axis is inconsequential since it is parallel to the grooves of the grating. Relative tilt resulting from relative rotation about the  $x$  axis can be used to compensate relative groove rotation. In addition, the out-of-plane shift, also referred to as the piston phase error, can be used to compensate the residual error caused by the finite space between two adjacent gratings. The

effect of piston misalignment was modeled thoroughly. Theoretical simulations show the far-field irradiance resulting from relative piston-type phase error between two tiled gratings (Fig. 96.3, calculation). A half-wave piston-type error causes the focal spot to split into two symmetric spots of equal energy and irradiance. Experimental verification of the predictions for

zero and half-wave errors indicates accurate control of the relative phase between the pair of tiled gratings as described below (Fig. 96.3, measurement). We experimentally observed that the majority of the focal-spot degradation occurs closer to the half-wave error, indicating a relative insensitivity in the vicinity of piston phase error, which is a multiple of  $2\pi$ .

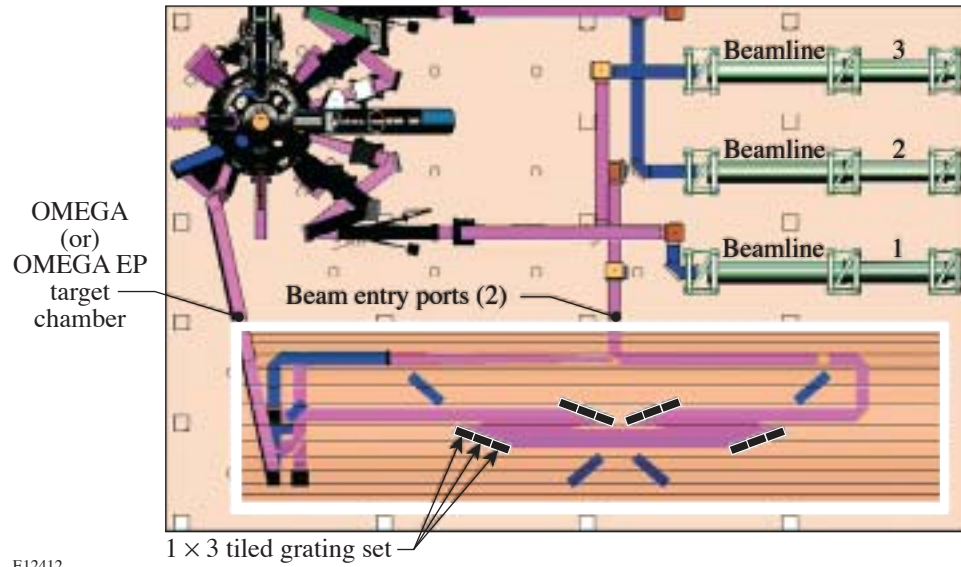


Figure 96.1

Tiled-grating compressors (TGC's) are capable of handling greater laser energy than a grating-aperture-limited compressor. For each of the gratings within a TGC,  $N \times M$  sub-aperture gratings can be adjacently mounted to form a larger tiled grating. Shown here is a four-grating compressor with each tiled grating containing three sub-aperture gratings. The aperture, and therefore the energy, is increased by a factor of  $N \times M$  over that of grating-aperture-limited compressors.

E12412

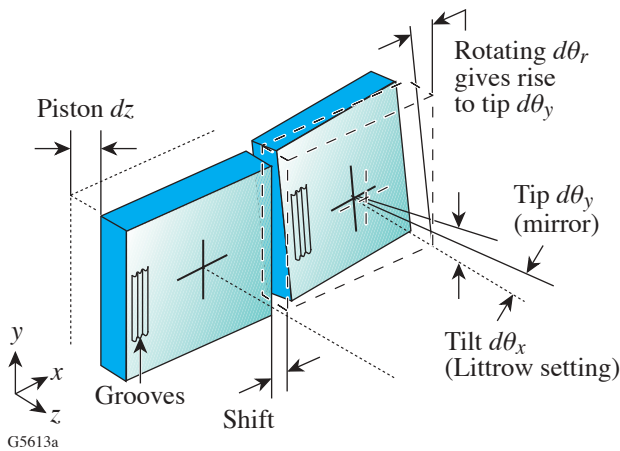
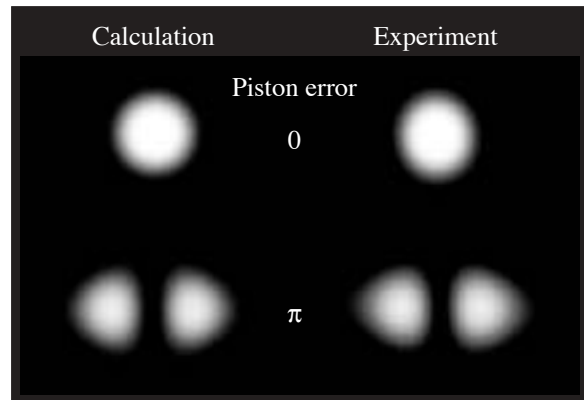


Figure 96.2

There are five degrees of freedom between each adjacent pair of gratings within a tiled-grating system. Relative shifts along the  $x$  and  $z$  axes result in a differential piston phase between the grating pairs. Similarly, relative rotations about the  $x$  and  $z$  axes result in a differential tilt between the grating pairs. Relative rotation about the  $y$  axis results in an additional tilt, while relative shift along the  $y$  axis is inconsequential since it is parallel to the grooves of the grating.



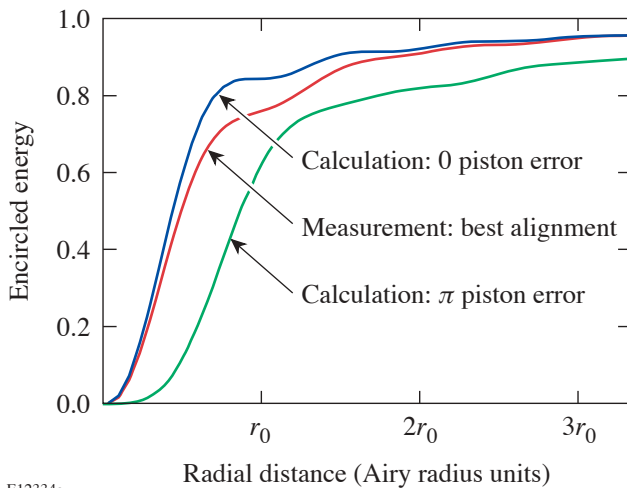
E12352

Figure 96.3

Theoretical simulations show the far-field effects from a relative piston phase error between two gratings. A  $\pi$ -phase shift causes the focal spot to split into two symmetric spots of equal energy and irradiance. Experimental verification of the predictions for zero and half-wave errors was achieved through accurate control of the relative piston.

## Experimental Demonstrations

The feasibility of precise grating tiling was first demonstrated with continuous-wave, monochromatic laser light. The tiled-grating assembly was located within a diagnostic package consisting of a Fizeau interferometer and a focal-plane sensor. An ADE Phase Shift MiniFiz,<sup>TM</sup> Model 100 interferometer contained a laser source that illuminated a pair of Jobin Ivon  $165 \times 220$ -mm gratings, with 1740 l/mm, set up in a Littrow configuration. The gratings were independently mounted within a precision assembly to achieve submicron positioning. A Zygo transmission flat, inserted into the Fizeau cavity, served as a beam splitter to pick off a portion of the beam reflected from the tiled grating. This beam was focused by a long-focal-length lens to form an aerial image. The image was magnified and relayed by an infinity-corrected,  $10\times$  microscope objective for far-field detection with a Spectral Instruments, Model 802, CCD camera. This diagnostic package provided accurate control of the phase front, thus allowing detailed studies of the focal-plane irradiance. As shown in Fig. 96.4, near-diffraction-limited performance was obtained with a pair of tiled gratings. The measured encircled energy, truncated at  $e^{-2}$  of the azimuthally averaged irradiance, was 0.89 with a Strehl ratio of 0.94. The measured focal-spot diameter was 1.2 to 1.3 times diffraction limited (XDL) as compared to an Airy-disc diameter corresponding to 84%



E12334a

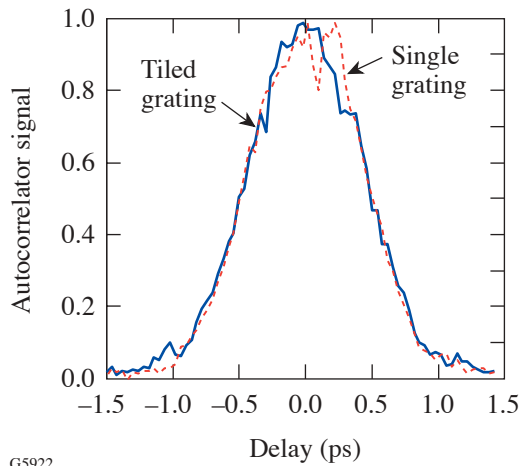
Figure 96.4

Near-diffraction-limited performance was obtained with a pair of tiled gratings. The measured encircled energy, truncated at  $e^{-2}$  of the azimuthally averaged irradiance, was 0.89 with a Strehl ratio of 0.94. The measured focal-spot diameter was 1.2 to 1.3 times diffraction limited (XDL) as compared to an Airy-disc diameter corresponding to 84%

encircled energy. For reference, the focal spot resulting from a  $\pi$  piston error is theoretically calculated to be 2.4 XDL. The small departure from theoretical predictions of ideal alignment is attributed to the cumulative wavefront error of the optics.

A demonstration of precise grating tiling was achieved by high-fidelity pulse compression within a CPA laser. The autocorrelation trace, corresponding to a Fourier-transform-limited, 650-fs, CPA laser pulse, was maintained after including a tiled-grating pair. A Positive Light laser consisted of a positively chirped, Time-Bandwidth GLX-200,<sup>TM</sup> mode-locked oscillator followed by a Spitfire,<sup>TM</sup> Ti:sapphire, regenerative amplifier. The amplifier output was a linearly chirped, nanosecond pulse with 250 ps/nm. The laser was operated at 540 Hz with 350  $\mu$ J per pulse without subsequent amplification. In normal operation the output pulse was compressed with a two-grating, two-pass compressor consisting of gold gratings with 1740 grooves per millimeter. For our demonstration of a TGC, the first grating, and necessarily the last grating in the compressor, was replaced by two tiled gratings with the same line spacing.

In a two-pass grating compressor, only the second and third gratings intercept a beam with spatial chirp of its spectrum. Both the physical gap between tiled gratings and the obscuration at the edge of each grating, where excessive wavefront gradients may need to be masked, give rise to modifications of the spectrum that can potentially cause pulse-shape distortion. Modeling of a partially dispersed beam propagated through an accurately tiled grating indicates that the primary effect from grating-to-grating gaps is pulse broadening. The percentage of broadening is approximately equal to the product of the beam-normalized gap width and beam-normalized spectral separation. For the large laser systems for which this research is aimed, this product is at most only a few percent. For the laser system used to demonstrate grating tiling, however, pulse-width broadening would have exceeded 50%; thus, accurate control of piston and tilt control would have been masked by unrelated obscuration effects. For this reason, only the first (fourth) grating was tiled. Construction of an all-tiled grating compressor is in progress and will be the subject of a future publication. A scanning, far-field autocorrelator was used to measure the compressed temporal pulse. As shown in the autocorrelation traces of Fig. 96.5, negligible pulse broadening and distortion were measured. Accurate control of the relative position of the tiled gratings, as well as accurate alignment of the TGC, resulted in compressed pulses of the same quality as those generated from a conventional grating compressor.



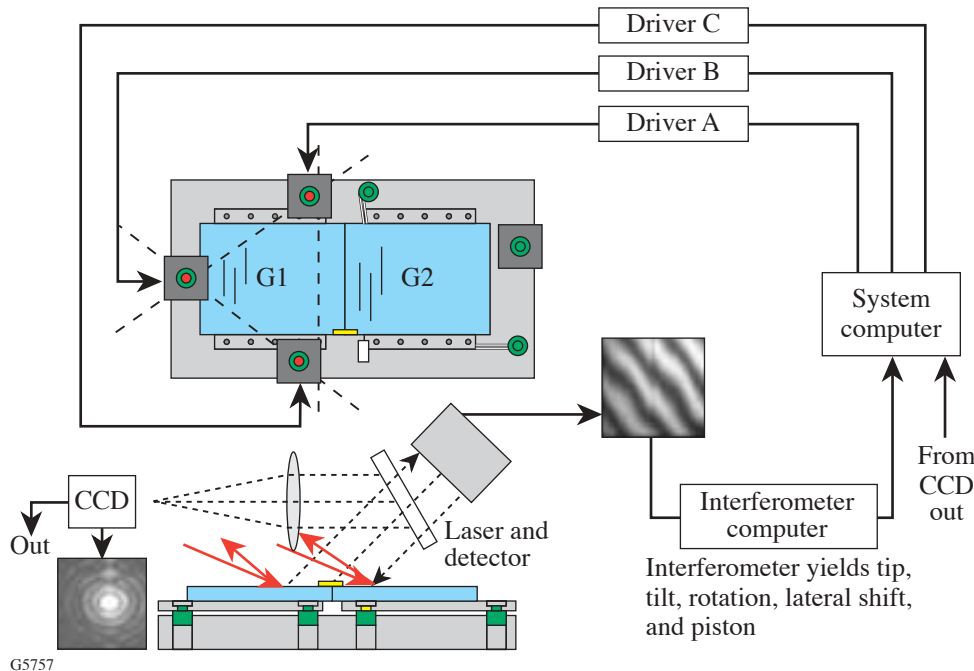
G5922

Figure 96.5  
The autocorrelation trace, corresponding to a Fourier-transform-limited, 650-fs, CPA laser pulse, was maintained by replacing a single compression grating with a tiled-grating assembly. Negligible pulse broadening and distortion, as shown in the autocorrelation traces, indicate accurate control of the relative positioning of the tiled gratings as well as accurate alignment of the grating compressor.

A test bed for mounting and aligning a reduced-scale TGC for the OMEGA EP laser system is in progress. Schematically illustrated in Fig. 96.6, the tiled-grating system incorporates currently available pointing, sensor, and positioning technology. In particular, flexure mounts provide optimal characteristics for grating mounts. While flexures offer high mechanical stiffness to carry the weight of the grating substrates, they allow extremely fine motion control in the orthogonal direction. In addition, spatial synchronous phase detection can be used for accurate interferometry to monitor differential piston and tilt.

**Conclusion**

In conclusion, our investigations of coherently combined gratings have resulted in the demonstration of subpicosecond-pulse compression using tiled gratings. A Fourier-transform-limited, 650-fs, CPA laser pulse was maintained by replacing a single compression grating with a tiled-grating assembly. Despite the perceived difficulty, we have developed a far-field-based approach that makes grating tiling practicable. We anticipate that, in conjunction with future improvements in grating size and damage threshold, the tiled-grating compressor will significantly increase the energy and irradiance available in high-energy, short-pulse lasers.



G5757

Figure 96.6  
Tiled-grating systems incorporate currently available technology for mounting and alignment. Mechanical flexures provide extremely fine motion control for relatively heavy grating substrates. The interferometer yields tip, tilt, rotation, lateral shift, and piston information.

## ACKNOWLEDGMENT

This work was supported by the U.S. Department of Energy Office of Inertial Confinement Fusion under Cooperative Agreement No. DE-FC03-92SF19460, the University of Rochester, and the New York State Energy Research and Development Authority. The support of DOE does not constitute an endorsement by DOE of the views expressed in this article.

## REFERENCES

1. D. M. Pennington, C. G. Brown, T. E. Cowan, S. P. Hatchett, E. Henry, S. Herman, M. Kartz, M. Key, J. Koch, A. J. MacKinnon, M. D. Perry, T. W. Phillips, M. Roth, T. C. Sangster, M. Singh, R. A. Snavely, M. Stoyer, B. C. Stuart, and S. C. Wilks, *IEEE J. Sel. Top. Quantum Electron.* **6**, 676 (2000).
2. P. Maine *et al.*, *IEEE J. Quantum Electron.* **24**, 398 (1988).
3. L. Li and J. Hirsh, *Opt. Lett.* **20**, 1349 (1995).
4. B. W. Shore *et al.*, *J. Opt. Soc. Am. A* **14**, 1124 (1997).
5. K. Hehl *et al.*, *Appl. Opt.* **38**, 6257 (1999).
6. B. Touzet and J. R. Gilchrist, *Photonics Spectra* **37**, 68 (2003).
7. T. Zhang, M. Yonemura, and Y. Kato, *Opt. Commun.* **145**, 367 (1998).
8. C. Pizarro *et al.*, *Appl. Opt.* **41**, 4562 (2002).
9. T. J. Kessler, J. Bunkenburg, and H. Huang, "Grating Array Systems for the Alignment and Control of the Spatial and Temporal Characteristics of Light," U.S. Patent Application (filed May 2003).
10. T. J. Kessler, J. Bunkenburg, H. Huang, A. Kozlov, C. Kelly, and D. D. Meyerhofer, "The Coherent Addition of Gratings for Pulse Compression in High-Energy Laser Systems," to be published in *Inertial Fusion Sciences and Applications 2003* (Elsevier, Paris, 2004).

